

The Comparison of Dry Hydrostatic Delay Measurement from GPS Ground-Based and Space-Based Receiver

Rohaniza M. Zali^{1,2,*} and Mandeep J. S.²

¹Department of Electrical Engineering, Politeknik Sultan Salahuddin Abdul Aziz Shah, Malaysia

²Department of Electrical, Electronic and System, Faculty of Engineering and Built Environment, UKM, Malaysia
Email: reeza79@yahoo.com (R.M.Z.); mandeep@ukm.edu.my (M.J.S.)

*Corresponding author

Abstract—Tropospheric delay is a significant cause of the Global Navigation Satellite System's (GNSS) services degrading, particularly when it comes to the geodetic estimation of coordinates on the surface of the planet. To quantify the delay brought on by the abnormalities in the tropospheric layer, researchers have employed a variety of methods. Since Global Positioning System Radio Occultation (GPS-RO) systems and the Global Positioning System (GPS) ground network estimate the tropospheric delay differently, we examined this measurement difference in this study. Therefore, this study has been performed to analyze the dry delay measurement from the ground-based station and validate it with the reprocessing data from the space-based station to understand the correlation of measurement between these two methods. The MetopA gave the worldwide delay data, while the 92 SuomiNet Network GPS stations, which cover the majority of the United States region, provided their measurement of the delay utilizing the element of slant water along the GPS ray while the MetopA provided the global data with around 150 selected data per day and analysis was conducted for the data in the year 2020. Hence, due to the difference in spatial data distribution between these two types of data, the mean value has been measured for each of the latitude zones, the result shows the minimum bias of 0.67 cm and RMSE 4.51 cm at the -30° to -60° and the maximum bias of 3.74 cm and RMSE 25.1 cm at the 30° to 60° latitude. Overall bias and Root Mean Square Error (RMSE) are 1.41 cm and 23.2 cm respectively which shows a good agreement between space-based and ground-based measurement that will help for better error modeling development in the future.

Keywords—Global Positioning System (GPS), tropospheric delay, refractivity, radio occultation, atmospheric

I. INTRODUCTION

The electromagnetic signal used in the Global Positioning System (GPS) propagates and travels through the Earth's atmosphere to the receiver, which can be installed in a variety of locations and experiences an atmospheric delay. Variations in atmospheric characteristics bring it on, and the signal's speed will also

alter [1, 2]. The delay caused by an error in the signal will affect most satellite GPS applications, especially in space geodesy, such as sea-level monitoring, earthquake-hazard mitigation, and any applications where the highest possible position accuracy is needed [3]. Hence, better measurement and modelling of errors is therefore essential. Nonetheless, we are encouraged to analyze the delay measure from different sources to see the correlation between the measurements. The majority of satellite GPS applications will be impacted by the delay brought on by a signal error. This is because a signal is reflective when it travels through the atmosphere, particularly in the troposphere layer where there is a significant concentration of gases and water vapor. Furthermore, both the optical and radio ranges are crucial for the tasks to calculate the tropospheric refractive index profile [4–6]. The assessment of refractivity is highly considered to increase target tracking and navigation accuracy because refractivity variation is stronger in the vertical than the horizontal [1, 7].

Additionally, numerous methods have been used by researchers to quantify signal errors, anticipate climate change, and monitor the ocean surface using a variety of data types. The majority of atmospheric monitoring data can be gathered either by a receiver on a local ground station or by a receiver in space using the GPS Radio Occultation (GPS-RO) approach. A recent study has been conducted by comparing the hydrostatic delay measured from the local GPS station with radiosonde data [8]. It shows a good correlation with the RMSE of 24.1 mm. Nonetheless, this study will focus on the analysis by using GPS-RO data due to the inexpensive and higher spatial distributions of data compared to the radiosonde data. In the technique, the signal's bending angle, which is produced by the GPS-RO technology and used to analyze atmospheric profiling data, has been measured [7, 9]. As a result, estimates of additional atmospheric factors like temperature and pressure have been made using the Abel transform [10]. Radio occultation technique has been applied for the limb sounding of the Earth's atmosphere

from Low Earth Orbit (LEO) [11] and it is also used in various ways, especially in weather forecasting. It also provides data with very high vertical resolution and global distribution, making it suitable for global monitoring. While the SuomiNet network is a GPS network developed by the National Science Foundation (NSF) of the United States with participation from various universities and institutions, nearly 103 SuomiNet sites have been established [12]. It is suitable for localization monitoring, particularly above-the-ground surface monitoring, but it is uneconomical if we want to increase the spatial resolution of the data coverage.

One of the factors causing the GPS signal to be delayed is the tropospheric delay. It might result from a signal traveling in a straight line from the satellite to the receiver, passing through the atmosphere, and then turning into a curve due to refractivity. Two terms—dry delay and wet delay—can be used to describe the entire tropospheric delay [2]. The dry delay is brought on by the atmosphere's dry gases, but the wet delay is brought on by the water vapor present, particularly near the bottom of the troposphere layer [13]. Approximately 90% of the total tropospheric delay is given by the dry elements. The remaining 10% is due to water vapor concentration, which can reach 35cm in humid regions and cannot be precisely modeled with the surface of measurement [14]. Because of its dependence on surface pressure and temperature, the dry delay, also known as the hydrostatic delay, has a smooth, slow variation in time [15]. Also measured dry delay using dry air refractivity along the vertical path from radiosonde data [11]. Due to the uncertainty in the amount of water vapor present in the estimation, the researchers proposed calibrating Dry Zenith Delay (DZD) from the existing Zenith Hydrostatic Delay (ZHD) in this study. The dry temperature data has been filtered out to the designated temperature limit since researchers [12, 16] believe that water vapor can be neglected at temperatures below 250K. As a result, in this study, we would like to compare the DZD measurement performance of GPS-RO and SuomiNet dry delay products in order to determine the bias and root mean square values of these two types of measurements.

The next section will deliberate on how the analysis was conducted using the SuomiNet dry delay data and ZHD derived from the dry profile of MetopA. Hence, the performance of both methods can be shown in the result and analysis section. Finally, the conclusion will be stated in the last section.

II. METHODOLOGY

A. GPS Data

The GPS system, which consists of a constellation of 24 satellites distributed across various orbital planes and orbits approximately 20,000 km above the Earth's surface [9], has been widely used in a wide range of applications, most notably in climate change tracking and navigation systems. Long-term weather monitoring systems rely on monitoring atmospheric conditions as well as changes in the Upper Troposphere and Lower Stratosphere layer

(UTLS). Reliable precipitation prediction and estimation are especially important for a better understanding of patterns in global climate change caused by natural variability or anthropogenic impacts. [12]. In the current study, the GPS system is used in a variety of ways, including radiosonde, GPS Ground-based receiver, and GPS RO, each with its own strengths in data collection and analysis processes.

In this study, we used the data collected from the SuomiNet network for the year 2020 as a set of ground-based GPS receivers with a specific location of coordinate with the real-time data estimation of atmospheric delay, and other atmospheric profiling through the lower atmosphere layer zone [17]. The radio occultation data from the MetopA mission with the spatial global distribution data from the single space-based GPS LEO receiver at the location of 824 kilometers above the surface of the earth, which observes over 500 occultation data per day [11], in order to measure tropospheric delay. The distribution data for SuomiNet network and MetopA can be shown in Fig. 1. We need to take into consideration the vertical data distribution with a range of up to 40km height and a precision of 0.1km for the determination of tropospheric dry delay from Radio Occultation (RO) data. For many years, researchers have used this RO technique to develop climate change monitoring measurement tools. This is because of the high accuracy and vertical resolution for global coverage.

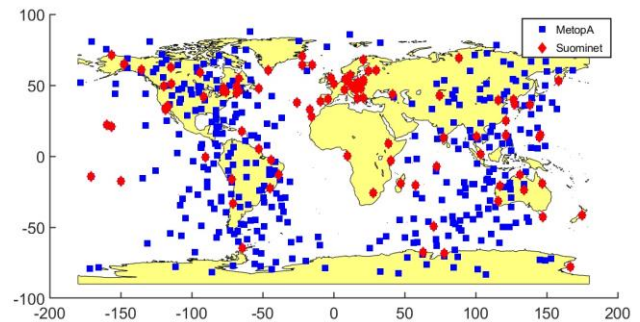


Fig. 1. The global distribution of data for Suominet and MetopA.

Fig. 2 shows the analysis of measurements for tropospheric delay from the ground-based real-time data collected and compared with the post-processing data from the RO mission. Real-time dry delay data has been made available via the SuomiNet network and has been extracted from the University Corporation for Atmospheric Research (UCAR) via www.unidata.ucar.edu. Therefore, we want to compare the measurement with the RO post-processed data in order to determine the validity and accuracy of the real-time dry delay measurement. The METOPA data can be archived via <https://data.cosmic.ucar.edu/gnss-ro/metopa/postProc/>. Due to the global distribution of RO data, the range of latitude has been filtered out to get the closest latitude location for both space-based and ground-based locations as shown in Fig. 1. The dry delay has been calculated using dry atmospheric profiling, which is the temperature (T), refractivity (n), and pressure (p) from the RO data with the

specific latitudinal, which is known as ZHD. By neglecting the water vapor content, ZHD contributes up to 90% of total tropospheric delay [16] and has remained stable over time. Suominet's processing data as a network of GPS ground-based stations provided the dry delay data estimation [15]. Additionally, the data were compared to determine the similarity and correlation between these two techniques.

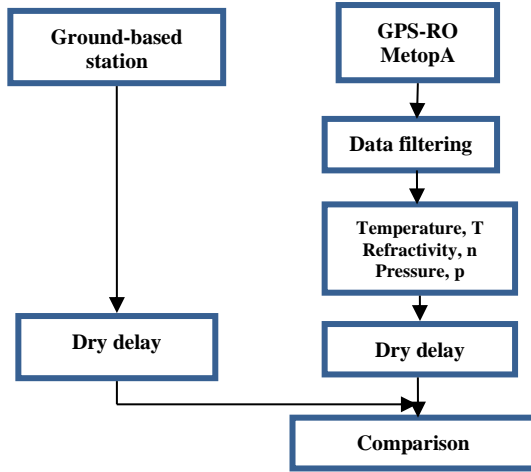


Fig. 2. Dry delay estimation process from GPS space-based and GPS ground-based data.

B. Tropospheric Delay

The GNSS signals propagate through the atmosphere layer and are received by the receiver located either in space at the LEO location known as GPS-RO or at the ground will pass through the ionosphere and also the lower atmosphere layer. However, the higher refractivity due to the irregularities factors in the troposphere layer causes the delay of the signal and leads to the degradation of the GPS navigation systems. As for the measurement of dry delay by the SuomiNet Network, the Precipitation Water Vapor (PW) has been considered as a product of Zenith Delay (ZD) which is based on the assumption that the atmosphere is azimuthally homogenous that gives an average zenith delay from which the hydrostatic or dry component from surface pressure is subtracted [17]. However, there is no further processing of data required from the SuomiNet GPS network which already provides real-time dry delay data that can be accessed directly from their database.

Furthermore, in this analysis, we will compare the measurement of Dry Delay from the GPS Network with the refractivity profile from the GPS RO reprocessing data which measured the tropospheric dry delay by using the concept of the deterministic least-square technique and Kalman filtering [2]. The dry delay term can be defined as a phase delay caused by the refractivity from the air and it was significant for measurement between the upper troposphere and stratosphere in which the presence of water vapor can be neglected [18, 19]. Therefore, in this study, the dry delay from occultation data will be estimated by using the dry refractivity (N_d) profile measured in parts

per million [ppm] with considering the location of the troposphere-stratosphere layer up to 30km height and assuming that the atmosphere is in hydrostatic equilibrium condition [2]. The dry delay, d [meters] can be estimated from the dry part of atmospheric refractivity [20–22] as shown in Eq. (1).

$$N_d = k \left(\frac{P_d}{T} \right) Z_d^{-1} \quad (1)$$

$$d = 10^{-6} k \int_{h_1}^{h_2} \frac{P_d(h)}{T(h)} Z_d^{-1} dh \quad (2)$$

$$Z_d^{-1} = 1 + P_d \left[(57.90 \times 10^8) \left(1 + \frac{0.52}{T} \right) - (9.4611 \times 10^{-4}) \frac{1}{T} \right] \quad (3)$$

where k is the hydrostatic constant for the dry element with the value 77.604 ± 0.014 K/mbar [23], P_d is the dry pressure (mbar), T is the dry temperature (Kelvin), and Z_d^{-1} is an inverse compressibility factor for dry air (K/mbar). We set the limits h_1 and h_2 as minimum and maximum levels due to the height of the troposphere-stratosphere layer from the surface of the earth. The dry pressure and temperature along the vertical path provided by occultation data were used to calculate the dry air refractivity along the vertical path [20]. Due to the calibration measurement of dry delay, DZD was mentioned as followed by Eq. (4), [14].

$$\Delta dry = \delta + \mu \frac{P_d}{T_d} + \varepsilon \quad (4)$$

where, δ and μ represent the bias and calibration scale factor respectively with the value of 12.20 ± 0.26 cm and 3.153 ± 0.077 cm K mbar⁻¹, while ε denotes a random disturbance which was neglected in this study.

Furthermore, in this study, we analyzed the Bias and Root Mean Square Error (RMSE) values to find the accuracy of the measurement. This can be obtained from Eqs. (5–6) respectively [22, 23].

$$Bias = \frac{1}{n} \sum_{i=1}^n (\hat{x}_i - x_i) \quad (5)$$

$$RMSE = \sqrt{\frac{1}{n} \sum_{i=1}^n (\hat{x}_i - x_i)^2} \quad (6)$$

where, n is to represent the number of observation data, \hat{x}_i is a ground-based delay measurement, and x_i is a space-based derived benchmark.

III. RESULT AND DISCUSSION

The 2020 GPS Network (Suominet) real-time data distribution with 26,356 dry delay data has been used in this study to conduct the analysis. The microwave propagation signal with the frequency of 1.6 and 1.2GHz (L1 and L2) from the GNSS to the ground/space receiver will pass through the atmosphere and suffer the degradation signal due to the delay caused by atmospheric elements. We already know that the upper troposphere's

dry fraction of the gases, which are responsible for the atmospheric delay, causes the dry component [14, 24]. Based on the Earth’s observation station’s latitude and longitude, the dry delay distribution is shown in Fig. 3 for comparison. The site of 14.330S, 170.70W recorded the largest mean dry delay with a value of 2472mm, whereas the lowest mean value was at 77.84°S, 166.7°E with a value of 2067 mm.

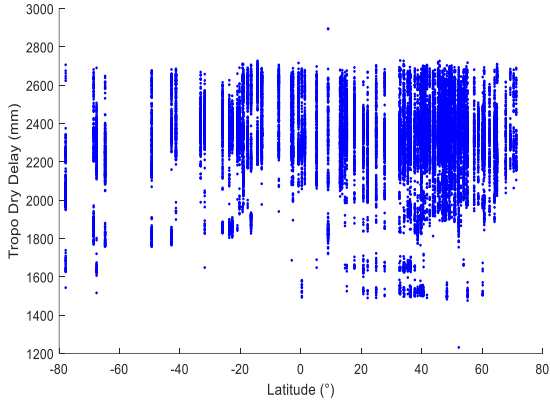


Fig. 3. Ground-based dry tropospheric delay with latitude.

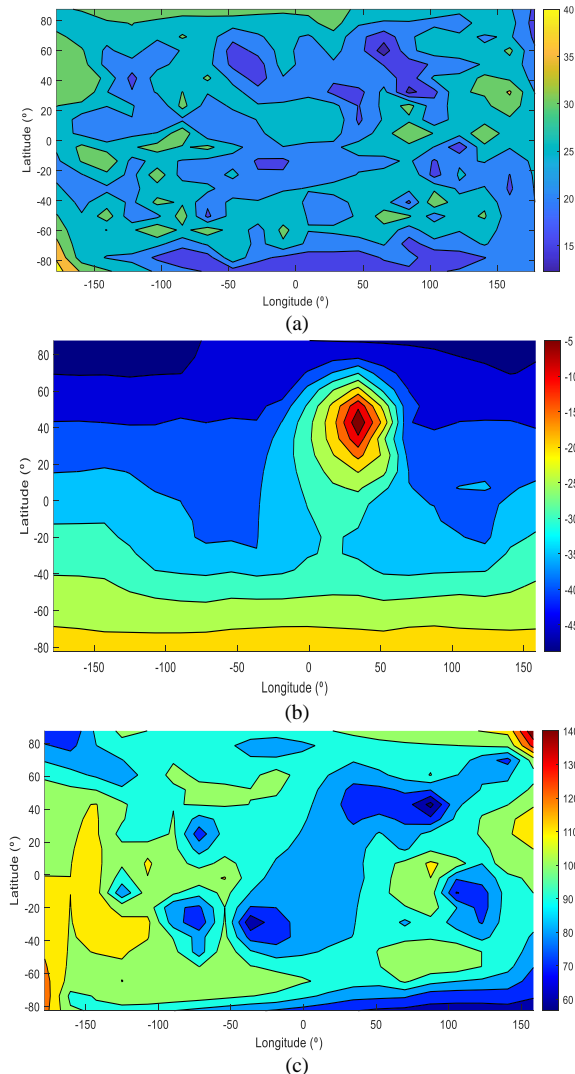


Fig. 4. Spatial distribution of (a) Refractivity, N, (b) Temperature, T (°C), and (c) Pressure, P (mbar) from RO data over 2020.

In the meantime, based on the chosen position close to the ground-based data distribution, the dry refractivity, N, dry temperature, and pressure profile from the space-based (RO) MetopA have been retrieved appropriately. Fig. 4 illustrates the spatial data distribution of refractivity, temperature, and pressure profile for the year 2020, showing that the Southern Hemisphere zone has the highest mean refractivity profile at 38.8021 and the Northern Hemisphere zone has the lowest at 8.57 at mid-latitude.

Despite this, the mean temperature distribution exhibits a trend of temperature variation from the Southern to Northern Hemispheres with the increment value from -46.4°C to 11.24°C which the hottest area was captured at mid-latitude zone 41.64°N , 42.52°E . Consequently, Eqs. (1–3) were utilized to predict the dry delay using the atmospheric data profiling that was retrieved from the reprocessing data. The study revealed a linear correlation with an R^2 of 0.7654 between the measurement of a dry delay from the GPS-RO and the ground-based approach. The bias measuring range has a minimum difference of 0.67 cm and a maximum difference of 3.74 cm. However, Fig. 5 below demonstrates that both measurement methods for determining the dry delay had a linear tendency.

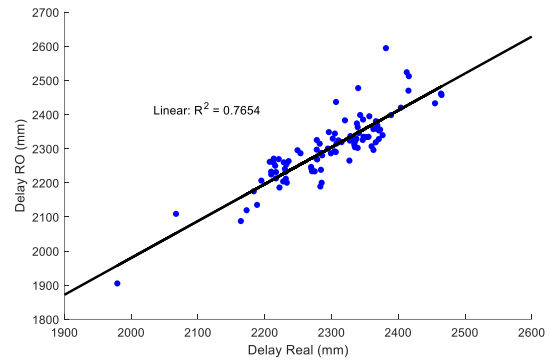


Fig. 5. The correlation measurement between GPS space-based receiver and ground-based receiver station.

TABLE I. MEAN DRY MEASUREMENT BASED ON THE LATITUDINAL ZONE

Latitude Zone (°)	Mean Dry Delay (cm)		Bias (cm)	RMSE (cm)
	Ground	Space		
60 to 90	230.9	231.1	0.96	6.41
30 to 59	230.4	229.5	3.74	25.1
0 to 29	230.7	228.8	1.05	7.05
-29 to 0	236.8	238.0	1.31	8.73
-59 to -30	233.1	231.2	0.67	4.51
-90 to -60	215.0	209.7	0.76	5.07

Nonetheless, different measurement performances can be found for different latitudinal zones. Table I displays the mean dry delay measured for the six different latitude zones of the Northern and Southern Hemispheres, respectively. According to the results of the analysis, the minimum bias is 0.67 cm and the RMSE is 4.51 cm at the -30° to -60° latitude and the maximum bias is 3.74 cm and

the RMSE is 25.1 cm at the 30° to 60° latitude. Overall bias, RMSE, and R^2 are 1.41 cm, 23.2 cm, and 0.7654 respectively. Generally, the analysis can show the robustness of the dry delay measurement using both ground-based and space-based GPS stations with a good correlation between them (see Table I).

In order to determine the trend of dry delay spatial data distribution, the investigation has continued by measuring the dry delay utilizing atmospheric profiling from the GPS-RO. Fig. 6 displays the average tropospheric dry delay's spatial distribution globally. According to the analysis findings, the equatorial zone had the driest delay at 1.593°S, 24.2125°E with a delay of 257.2 cm which is a difference of 147.4cm from the lowest delay that has been recorded at the 82°N, 155.4°E. The average tropospheric dry delay is 229.2 cm which has been recorded for most places.

Furthermore, the measurement of the dry delay for the entire year of 2020 can be seen in Fig. 7 on a daily basis for both GPS ground-based and GPS RO measurements. According to Fig. 7(a), the average delay for data distribution recorded by 92 GPS ground-based stations is 230.3 cm, with the shortest delay being 123.18 cm on February 13th at the location of 52.30 N, 10.50E and the longest delay being 289.4cm on January 4th at the location of 9.030N, 38.80E. In July, the shortest mean delay was recorded in 77.840S and 1660E, with a value of 206.7cm. Thus, the GPS RO measurement with 439 selected satellite coordinates as shown in Fig. 7(b) involves 144,187 data that have been measured, the minimum value of dry delay is 102.9 cm at the location 60°N, 158°E while the maximum delay is 274.1 cm at 57.7°N, 87.2°W. The lower dry delay for the whole year was also recorded in the equatorial zone for both hemisphere zones at the range of $\pm 0^\circ$ to $\pm 16^\circ$ latitude.

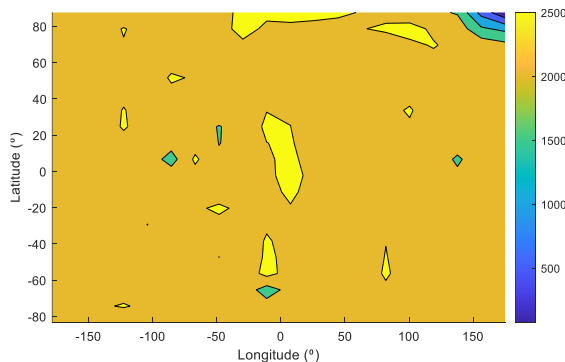
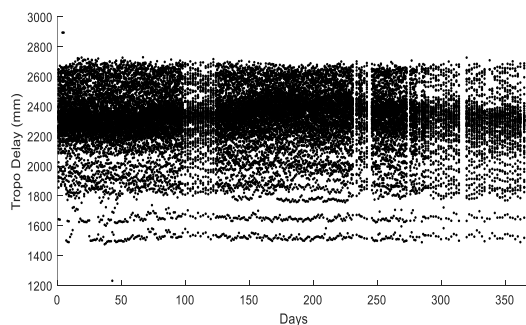
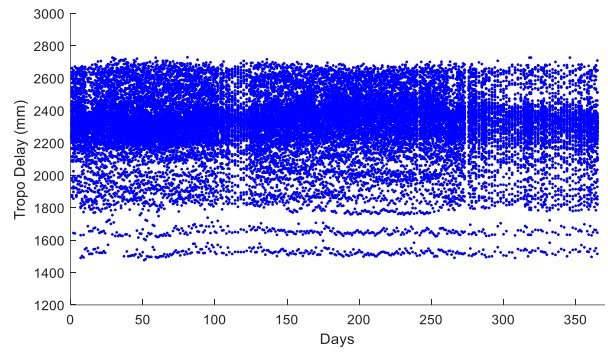


Fig. 6. Spatial distribution of tropospheric delay.



(a)



(b)

Fig. 7. The measurement of Tropospheric dry delay for the year 2020 (a) GPS ground-based (b) GPS RO.

IV. CONCLUSION

Due to the signal's refraction as it travels through the atmospheric layer, the GPS system has experienced signal lag. The signal that travels from the GNSS transmitter to the GPS receiver, which is situated either in low earth orbit or on the ground, can be utilized to estimate the delay of a signal brought on by refractivity. Both ground-based and space-based receivers are capable of receiving the signal, although the ground-based receiver obviously has more restrictions due to the higher cost of construction and the fewer stations it can support. Despite this, the ground-based GPS receiver's spatial distribution limitation makes the GPS space-based receiver a better choice for estimating global distribution data.

In general, this study has compared the post-processing data from GPS-RO with the measurement and performance of tropospheric dry delay from ground-based receivers. The study demonstrates a linear association between tropospheric dry delay estimation using measurements taken from the space station and the ground station. With a bias of 1.41 cm, it demonstrates that SuomiNet and GPS-RO perform well in estimating the global GPS signal delay. Therefore, based on the findings of this work, more precise models for improved tropospheric delay measurement can be created in the future. However, the wet delay term, which should be carefully considered notably for the lower layer of the troposphere, which is up to 100m above the surface of the planet, was outside the purview of this study. This is because a higher refractive value in the lower troposphere layer may result from a larger concentration of water vapor as well as gases from anthropogenic activity.

CONFLICT OF INTEREST

The authors declare no conflict of interest.

AUTHOR CONTRIBUTIONS

Rohaniza M. Zali has conducted the research, data collection, conception of the work, data analysis and interpretation, and drafting of the article. By contrast, Mandeep J. S was doing the critical revision of the article. All authors have approved the final version.

ACKNOWLEDGMENT

We would like to thank UCAR for providing MetOpA and SuomiNet data through their URL link of www.unidata.ucar.edu, as well as the Malaysian Ministry of Higher Education and the National University of Malaysia for their assistance with my research study.

REFERENCES

- [1] X. Dong, F. Sun, Q. Zhu, L. Lin, Z. Zhao, and C. Zhou, "Tropospheric refractivity profile estimation by GNSS measurement at China big-triangle points," *Atmosphere (Basel)*, vol. 12, no. 11, 2021. doi: 10.3390/atmos12111468
- [2] S. Nistor and A. S. Buda, "determination of zenith tropospheric delay and precipitable water Vapor using GPS technology," *Math. Model. Civ. Eng.*, vol. 12, no. 2, pp. 21–26, 2016. doi: 10.1515/mmce-2016-0007
- [3] V. C. Opaluwa, Y. D. Adejare, Q. A. Suleyman, Z. A. T. Abazu, I. C. Adewale, T. O. Odesanmi, and A. O. Okorocha, "Comparative analysis of five standard dry tropospheric delay models for estimation of dry tropospheric delay in GNSS positioning," *Am. J. Geogr. Inf. Syst.*, vol. 2, no. 4, pp. 121–131, 2013. doi: 10.5923/j.ajgis.20130204.05
- [4] A. N. Huthaifa, A. Raed, M. R. Steven, Y. Bettouche, A. Kouki, and B. Agba, "Long term evolution of the surface refractivity for arctic regions," *Radio Sci.*, vol. 54, no. 602–611, p. 11, 2022.
- [5] W. H. Lehn and S. D. V. Werf, "Atmospheric refraction: A history," *Appl. Opt.*, vol. 44, no. 27, pp. 5624–5636, 2005. doi: 10.1364/AO.44.005624
- [6] X. Liu, Z. Wu, and H. Wang, "Inversion method of regional range-dependent surface ducts with a base layer by doppler weather radar echoes based on WRF model," *Atmosphere (Basel)*, vol. 11, no. 7, 2020. doi: 10.3390/atmos11070754
- [7] S. Ge, "Gps radio occultation and the role of atmospheric pressure on spaceborne gravity estimation over antarctica presented in partial fulfillment of the requirements for the degree doctor of philosophy in the graduate school of the ohio state university by dis," *Sp. Weather Int. J. Res. Appl.*, no. 479, 2006.
- [8] L. Li *et al.*, "A new zenith hydrostatic delay model for real-time retrievals of GNSS-PWV," *Atmospheric Measurement Techniques*, pp. 6379–6394, 2021.
- [9] R. H. Ware *et al.*, "Suominet: A real-time national GPS network for atmospheric research and education," *Bull. Am. Meteorol. Soc.*, vol. 81, no. 4, pp. 677–694, 2000.
- [10] S. Businger *et al.*, "The promise of GPS in atmospheric monitoring," *Bull. Am. Meteorol. Soc.*, vol. 77, no. 1, pp. 5–18, 1996.
- [11] M. Bevis, S. Businger, T. A. Herring, C. Rocken, R. A. Anthes, and R. H. Ware, "GPS meteorology: remote sensing of atmospheric water vapor using the global positioning system," *Journal of Geophysical Research-Atmospheres*, vol. 97, no. 92, pp. 787–801, 1992.
- [12] S. A. M. Younes, "Modeling investigation of wet tropospheric delay error and precipitable water vapor content in egypt," *Egypt. J. Remote Sens. Sp. Sci.*, vol. 19, no. 2, pp. 333–342, 2016. doi: 10.1016/j.ejrs.2016.05.002
- [13] R. A. Phinney and D. L. Anderson, "On the radio occultation method for studying planetary atmospheres," *J. Geophys. Res.*, vol. 73, no. 5, pp. 1819–1827, 1968. doi: 10.1029/ja073i005p01819.
- [14] J. Mangum and P. Wallace, "Atmospheric refractive signal Bending and propagation delay," *Pasp*, vol. 127, no. 947, pp. 74–91, 2009.
- [15] Y. Liu, H. Baki Iz, and Y. Chen, "Calibration of zenith hydrostatic delay model for local GPS applications," *Radio Sci.*, vol. 35, no. 1, pp. 133–140, 2000. doi: 10.1029/1999RS900100
- [16] E. R. Kursinski, G. A. Hajj, J. T. Schofield, R. P. Linfield, and K. R. Hardy, "Observing earth's atmosphere with radio occultation measurements using the global positioning system," *J. Geophys. Res. Atmos.*, vol. 102, no. 19, pp. 23429–23465, 1997. doi: 10.1029/97jd01569
- [17] Z. Zeng, S. Sokolovskiy, W. S. Schreiner, and D. Hunt, "Representation of vertical atmospheric structures by radio occultation observations in the upper troposphere and lower stratosphere: Comparison to high-resolution radiosonde profiles," *J. Atmos. Ocean. Technol.*, vol. 36, no. 4, pp. 655–670, 2019. doi: 10.1175/JTECH-D-18-0105.1
- [18] M. Loiselet, N. Stricker, Y. Menard, and J. P. Luntama, "GRAS-MetOp's GPS-based atmospheric sounder," *ESA Bull.*, vol. 102, no. may, pp. 38–44, 2000.
- [19] U. Riccardi, U. Tammaro, and P. Capuano, "Tropospheric delay in the neapolitan and vesuvius areas (Italy) by means of A dense GPS array: A contribution for weather forecasting and climate monitoring," *Atmosphere (Basel)*, vol. 12, no. 9, 2021. doi: 10.3390/atmos12091225
- [20] P. Benevides, J. Catalão, P. Miranda, and M. J. Chinita, "Analysis of the relation between GPS tropospheric delay and intense precipitation," *Remote Sens. Clouds Atmos. XVIII; Opt. Atmos. Propag. Adapt. Syst. XVI*, vol. 8890, p. 88900Y, 2013. doi: 10.1117/12.2028732
- [21] G. A. Hajj, E. R. Kursinski, L. J. Romans, W. I. Bertiger, and S. S. Leroy, "A technical description at atmospheric sounding by GPS occultation," *J. Atmos. Solar-Terrestrial Phys.*, vol. 64, no. 4, pp. 451–469, 2002.
- [22] Y. Zhao, X. Liu, L. Liu, K. Pu, and K. Song, "Reconstruction of rainfall field using earth-space links network: A compressed sensing approach," *Remote Sens.*, vol. 14, no. 19, 2022.
- [23] D. Zhang, J. Guo, M. Chen, J. Shi, and L. Zhou, "Quantitative assessment of meteorological and tropospheric zenith hydrostatic delay models" Sciencedirec, *Adv. Sp. Res.*, 2016.
- [24] T. Schmidt, S. Heise, J. Wickert, G. Beyerle, and C. Reigber, "GPS radio occultation with CHAMP And SAC-C: Global monitoring of thermal tropopause parameters," *Atmos. Chem. Phys.*, vol. 5, no. 6, pp. 1473–1488, 2005.

Copyright © 2024 by the authors. This is an open access article distributed under the Creative Commons Attribution License ([CC BY-NC-ND 4.0](https://creativecommons.org/licenses/by-nc-nd/4.0/)), which permits use, distribution and reproduction in any medium, provided that the article is properly cited, the use is non-commercial and no modifications or adaptations are made.